Available online at www.sciencedirect.com
SCIENCE DIRECT®
Physics of the Earth and Planetary Interiors 149 (2005) 31–51
PHYSICS OF THE EARTH AND PLANETARY INTERIORS
www.elsevier.com/locate/pepi

Plate motions, slab dynamics and back-arc deformation

Arnauld Heuret*, Serge Lallemand

Laboratoire de Dynamique de la Lithosphere, Institut des Sciences de la Terre, de l'Environnement et de l'Espace de Montpellier (ISTEEM), CNRS—Université Montpellier 2, CC. 60, place E. Bataillon, 34095 Montpellier cedex 5, France

Received 12 September 2003; received in revised form 22 March 2004; accepted 26 August 2004

Abstract

Back-arc extension or compression is often related to a particular behavior of the slab (dip change and/or forward/backward migration) with respect to the upper plate. Slabs act, either passively when anchored in the deep mantle whereas back-arc deformation accommodates the backward or forward motion of the upper plate with respect to the trench; or actively when slab pull – increasing with slab age – forces the trench to rollback. In addition to these two mechanisms, i.e., slab anchor and slab rollback, numerous observations support the existence of dynamic mantle flow that can exert an overpressure on one side of the slab, causing its forward or rearward migration with respect to the arc.

Based on a compilation of upper plate absolute motion, trench absolute motion, back-arc deformation rate, upper plate strain regime and slab age for all oceanic subduction zones—excluding any kind of collision with continents, arcs or plateaus, we have examined how the combined effects of these parameters can account for the observed back-arc deformations. Our main results are: (1) a global correlation exists between upper plate absolute motion and back-arc deformation, i.e., back-arc extension when upper plate retreats and vice-versa; (2) there are as many advancing trenches as retreating ones, with trench motion globally limited to 50 mm y^{-1}; furthermore, there is no positive correlation between trench retreat and slab age; and (3) upper plate absolute motion often fails to explain the back-arc deformation rates and the trench motions observed at several subduction zones, as Tonga, New Hebrides, Sandwich or Ryukyu; we propose that the trench migration of these subduction zones are on the influence of mantle flows. We conclude that spontaneous trench rollback related to slab pull is negligible with respect to upper plate motion. Back-arc deformation regime is mostly controlled by the upper plate absolute motion relative to a partly anchored slab (trench motion is limited to 50 mm y^{-1}), even if locally, mantle flows force slab to move.

Keywords: Back-arc deformation; Plates absolute motion; Anchoring force; Slab pull force; Mantle flow

1. Introduction

Plate interaction in the subduction process often generates back-arc deformation. Along the 60,000 km of trench that run over the world, one can observe a great variability in the back-arc deforma-

* Corresponding author. Tel.: +33 467 143301; fax: +33 467 143642.
E-mail address: heuret@dstu.univ-montp2.fr (A. Heuret).

0031-9201/$ – see front matter
doi:10.1016/j.pepi.2004.08.022

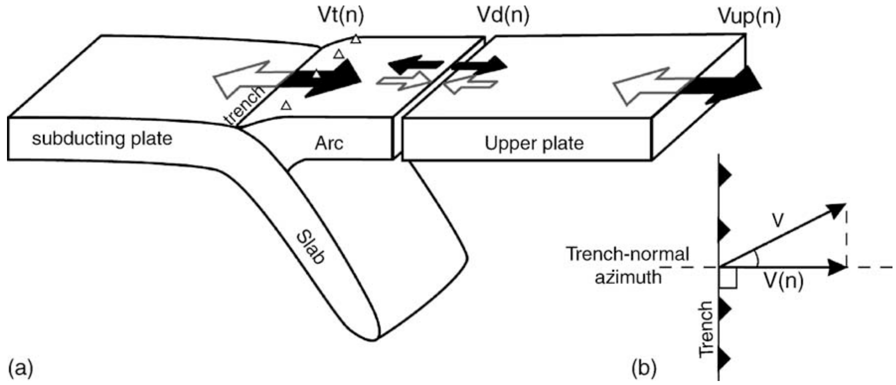

Fig. 1. (a) Structural pattern of subduction zones. V_{up}: upper plate absolute motion, V_t: trench absolute motion, V_d: back-arc deformation rate. Grey and black arrows, respectively, refer to positive and negative velocities. (b) Trench-normal components of motion estimate (V_{up}, V_t or V_d). V: rate; $V_{(n)}$: trench-normal component of rate.

tion style, from highly extensional (characterized by back-arc spreading and typified by the Mariana arc), to highly compressive (characterized by back-arc shortening and typified by the Chilean arc) (Uyeda and Kanamori, 1979; Uyeda, 1982). Understanding why back-arc tectonic style is tensional in some cases and compressive in others is still one of the main problems related to subduction zones dynamics.

The earliest attempts to explain back-arc deformation, and especially back-arc spreading, invoked mantle diapirism (e.g., Oxburgh and Turcotte, 1974) or secondary convection behind arc (e.g., Sleep and Toksöz, 1971), but models of these types were unable to explain the observed variability of back-arc deformation. Examination of the role of various subduction parameters, and in particular those of plate kinematics such as upper plate and trench absolute motions, appeared relevant in earlier studies (e.g., Jarrard, 1986; Garfunkel et al., 1986; Otsuki, 1989), although such studies sometimes led to contradictory conclusions. By making the simple assumption that internal forces, like gravitational collapse or back-arc ridge-push, are negligible in oceanic subduction zones (i.e., subducting plate is oceanic), the existence of back-arc deformation can be simply analyzed as a difference of motion between the upper plate (its undeformed and almost rigid part, as opposed to the back-arc deformed zone) and the subduction hinge (trench and subduction hinge are equally used to refer to the plate boundary): how do upper plates and trenches combine their respective absolute motions, V_{up} and V_t, to yield the observed deformations? (See Fig. 1 for a description of the main structural elements of the subduction system.) Does one of these motions dominate or do they contribute equally to the overall deformation rate V_d?

The main issue of our approach is the trench/slab dynamics. If upper plate motion can reach very important values (up to 90 mm y^{-1} for the Philippine Sea plate back of the Mariana subduction zone, in the HS3-NUVEL1A reference frame, Gripp and Gordon, 2002), how does trench react to this motion: does the subduction hinge follow the upper plate motion or does it resist this motion, generating back-arc deformation? Upper plate motion is not the only possible cause for trench to migrate. Indeed, in oceanic subduction zones, the subduction hinge is also affected by the negative buoyancy of the slab and is likely to migrate spontaneously away from the upper plate ("slab/trench rollback" refers to this spontaneous migration), inducing back-arc extension. In theory, one may also consider an additional pressure force on one side of the slab originating from asthenospheric flow (Shemenda, 1994). Such flow may cause slab migration in a direction normal to the trench (we will further describe the observations that support the existence of such mantle flow). These three possible trench behaviors are, respectively, described as the "upper plate motion controlled model", the "slab rollback model" and the "mantle flow induced model". The different forces that may affect trench motion are shown on Fig. 2.

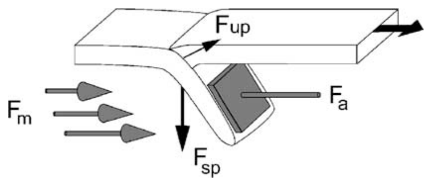

Fig. 2. Schematic cross section of a subduction zone, showing the main forces that may affect trench migration. F_{sp}: slab pull force, F_{up}: suction/pushing force related to the upper plate absolute motion and which acts on the plate interface, making the upper plate interdependent with the subduction hinge, F_a: slab anchoring force, F_m: pressure force generated by mantle flows on one side of the slab in the trench-normal direction.

1.1. The "upper plate motion controlled model"

Subduction hinge is affected by upper plate motion through two kinds of forces: (1) a suction/push force (F_{up}), which acts on the plate interface, making the upper plate interdependent with the subducting plate, and allowing upper plate motion to be transmitted to the top of the slab; and (2) the anchoring-force (F_a), which is the viscous resistance force opposed by the asthenosphere to any lateral migration of the slab and trench that may be induced by F_{up}. Following Scholz and Campos (1995), F_a can be described as the hydrodynamic force acting on the slab from the steady edgewise translation of an ellipsoid through a viscous fluid, which is given as a function of V_{up} and of the average mantle viscosity over the depth range of the slab (μ):

$$F_a = -6\pi\mu C V_{up} \qquad \text{(a)}$$

where C is a function of slab width and length.

The back-arc deformation results from the absolute motion of the upper plate with respect to a more or less fixed trench, i.e., from the balance between F_{up}, which tends to move the trench and F_a, which tends to resist this motion. Upper plate retreat relative to the more or less fixed trench induces back-arc extension, and upper plate advance gives rise to compression (Fig. 3). V_{up} determines the maximum value that both V_d and V_t could reach. Note that there are two distinguishable end-member cases: "perfectly anchored slabs""(the "anchored slab model" of Uyeda and Kanamori, 1979), for which the anchoring-force intensity is maximum, all the upper plate motion is converted into back-arc deformation ($V_d = V_{up}$) and the trench is fixed ($V_t = 0$); and, "perfectly free slabs", for which there is neither

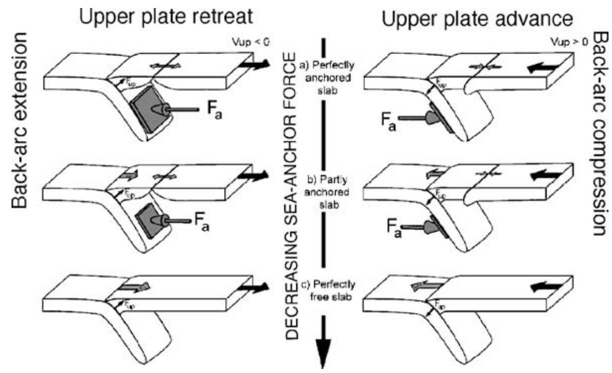

Fig. 3. The "upper plate motion controlled model". V_d: back-arc deformation rate, V_{up}: upper plate absolute motion, V_t: trench absolute motion, F_{up}: suction/pushing force related to the upper plate absolute motion and which acts on the plate interface, making the upper plate interdependent with the subduction hinge, F_a: slab anchoring force. (a) Perfectly anchored slab: trench is fixed (V_t: 0) and all upper plate absolute motion is converted into back-arc deformation (V_d: V_{up}). (b) Partly anchored slab: balance between upper plate absolute motion and both trench absolute motion and back-arc deformation rate ($V_d + V_t = V_{up}$) as a function of the anchoring force intensity. (c) Perfectly free slab: trench follows upper absolute motion ($V_t = V_{up}$) and no back-arc deformation occurs ($V_d = 0$).

anchoring-force nor back-arc deformation ($V_d = 0$), but a dominant F_{up} force and a trench that strictly follows the upper plate ($V_t = V_{up}$). Between these two end-member cases, subduction zones get "partly anchored slabs". Deformation rates and trench velocities are a function of anchoring-force efficiency and verify $V_{up} = V_t + V_d$.

To briefly summarize, if back-arc deformation and trench motion are dominantly controlled by the absolute motion of the upper plate with respect to a more or less fixed trench, we might expect that: (1) upper plate retreat is preferentially associated with back-arc extension and vice-versa for compression; (2) V_d increases with V_{up}; and (3) V_d and V_t could not exceed V_{up}.

1.2. The "slab rollback model"

The negative buoyancy of the subducted lithosphere with respect to the surrounding mantle (slab pull force, F_{sp}) is thought to be one of the main driving force of Earth's tectonic plates motion (e.g., Forsyth and Uyeda, 1975; Chapple and Tullis, 1977; Carlson et al., 1983). Following Carlson et al. (1983), slab pull force is slab

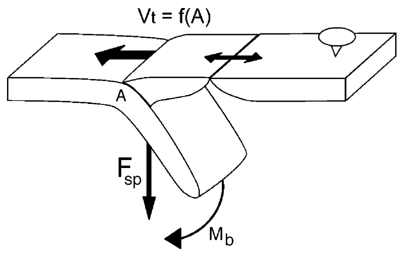

Fig. 4. The "slab rollback model". V_{up}: upper plate absolute motion, V_t: trench absolute motion, F_{sp}: slab pull force, M_b: bending moment, A: slab age. The upper plate is supposed to be fixed.

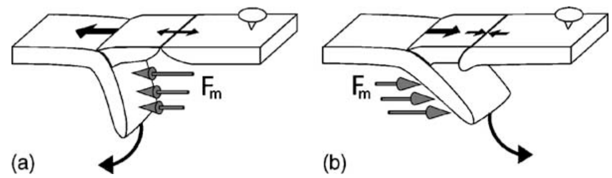

Fig. 5. The "mantle flow induced model". F_m: pressure force generated by mantle flows on one side of the slab in the trench-normal direction. The upper plate is supposed to be fixed. (a) Mantle flow and the associated F_m push on the upper plate side of the slab. Trench retreat and back-arc extension are generated. (b) Mantle flow and the associated F_m push on the subducting plate side of the slab. Trench advance and back-arc compression are generated.

age dependent:

$$F_{sp} = K\,\Delta\rho L A^{1/2} \tag{b}$$

where $\Delta\rho$ defines the density difference between slab and mantle, L is the slab length, A is the age of the slab and K is a constant.

The slab pull force and the associated bending moment (M_b) would generate a spontaneous seaward and slab age dependent (increasing with A) trench/slab migration, called "rollback", (e.g., Molnar and Atwater, 1978; Dewey, 1980; Garfunkel et al., 1986), and thus an extensional back-arc deformation (Fig. 4). According to this "slab rollback model" (1) seaward trench motion should be an ubiquitous feature of oceanic subduction zones; (2) the older and colder a slab is, the harder it should pull down on the hinge and the faster it should rollback; and (3) back-arc extension should be associated preferentially with old slabs.

1.3. The "mantle flow induced model"

The asthenospheric mantle that surrounds slabs and the flows that may drive it are another possible source for slab/trench migration (e.g., Shemenda, 1994): the additional pressure force (F_m) generated by such mantle flows on one side of the slab may cause slab translation in a direction normal to the trench (Fig. 5). One may consider three types of dynamic mantle flow acting on slabs (see arrows on Fig. 6): a global eastward flow possibly associated with the westward drift of lithosphere (e.g., Nelson and Temple, 1972; Doglioni, 1993), regional flows like the global escape tendency of sub-Pacific upper mantle as a result of the shrinking of the Pacific area (e.g., Garfunkel et al., 1986; Lallemand, 1998), and local flows like counterflows in the vicinity of retreating slab edges or tears (e.g., Alvarez, 1982; Russo and Silver, 1994; Yogodzinski et al., 2001).

1.4. Toward a statistical approach

In natural subduction systems (Fig. 2), the observed trench/slab migration velocity V_t, and upper plate deformation rate V_d, may result from a balance between the combination of all the forces that are able to drive trenches on the one hand (i.e., upper plate, buoyancy and mantle flow forces), and, the force that resist trench/slab migration on the other hand (i.e., the slab anchoring-force).

Despite the apparent complexity in the combination of the various forces' influences, previous statistical studies on subduction zones have provided encouraging results on the respective contribution of each effect, but also contradictory conclusions. The global correlation between mountain building and trenchward-advancing upper plates and between back-arc spreading and retreating upper plates (e.g., Hyndman, 1972; Chase, 1978), and the fact that among a set of 26 parameters tested by Jarrard (1986), V_{up} was found to be the best single predictor of strain regime, strongly point towards a dominant "upper plate controlled model" for back-arc deformation. However, some cases are inconsistent with an anchoring effect (Jarrard, 1986; Otsuki, 1989), but rather suggesting an additional driving mechanism for back-arc deformation and trench migration. Uncertainties on V_d and V_t led to contradictory conclusions on the nature of this secondary driving mechanism: Garfunkel et al. (1986) described a

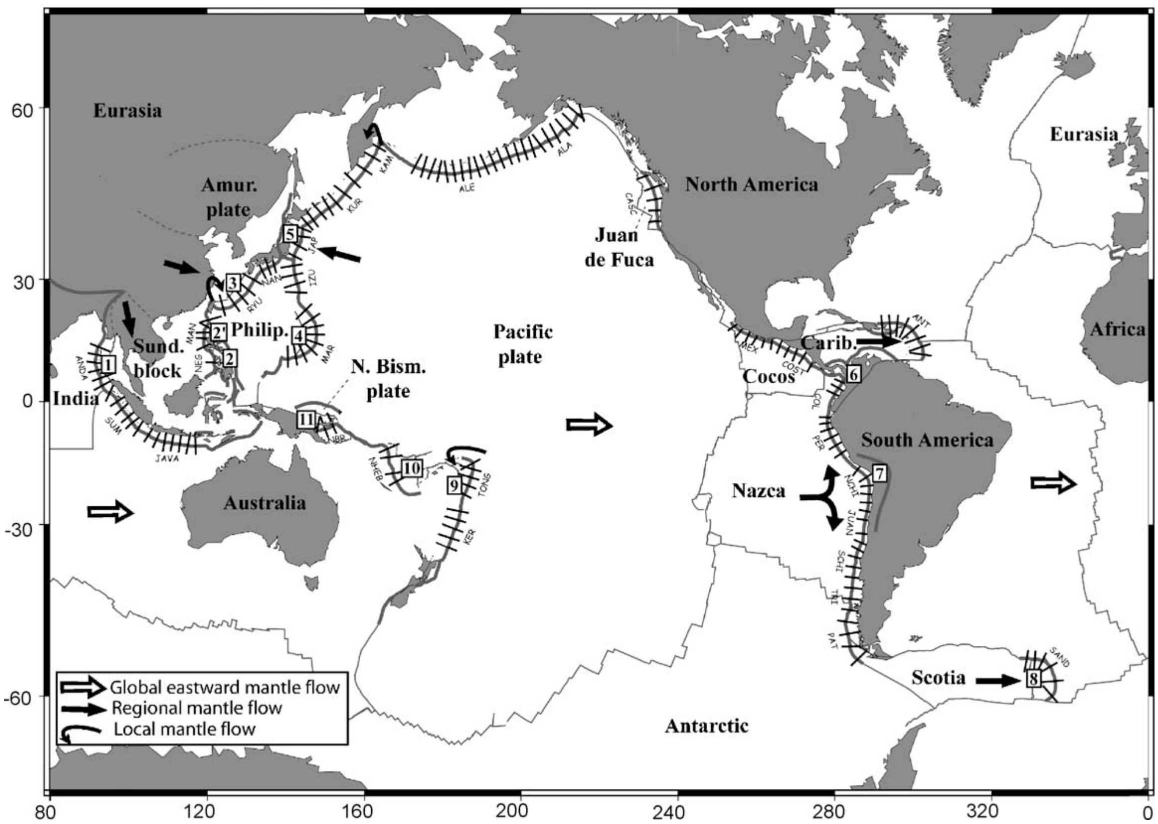

Fig. 6. Oceanic subduction zones in the world and major plate boundaries (with Sund. block: Sundaland block, Amur. plate: Amurian plate; N. Bism plate: North Bismarck plate). (1–12): the different "arc-blocks" used in the study; (1): Andaman Arc; (2): Visayas Block; (2′): Luzon Block; (3): Ryukyu Arc; (4): Mariana Arc; (5): Honshu; (6): North Andean Block; (7): Andes; (8) Sandwich Islands; (9): Tonga Arc; (10): New Hebrides Arc; (11): South Bismarck Plate. Thick gray lines indicate convergent plate boundaries (not only oceanic subduction zones but also those with abnormal subducting plates, i.e., continental lithosphere, volcanic arc, or oceanic lithosphere bearing oceanic plateaus). Oceanic subduction zones are systematically sampled. Sampled points are represented by black segments that cross the convergent boundary line. Thin black lines indicate divergent and strike-slip faulting plate boundaries. Abbreviations for subduction zones and references for plate and "arc-blocks" motions are in Table 1.

general trench rollback that increased as a function of slab age, whereas Jarrard (1986) found many advancing trenches, and no clear relation with slab age, and concluded that not only the slab rollback is globally negligible, but also that mantle flow effects were possibly important.

Since these earlier studies there has been a general improvement of available data, both in accuracy – especially with better constrained absolute reference frames and, above all, with much better estimated back-arc deformation due to the recent GPS data records – and in the homogeneity of data sources, with the advent of global datasets like ocean floor age that permit more rigorous comparisons between subduction zones. These improvements allow a new examination of the respective contribution of V_{up} and V_t to the overall back-arc deformation, and allow more stringent tests of whether or not slab anchoring is effective, whether a significant slab pull effect on trench motion is plausible, and whether evidence of mantle flow influences could be detected. To answer these questions, we test the consistency of the two most referenced driving mechanisms of back-arc deformation, i.e., "upper plate motion controlled" and "slab rollback" models, considering a "passive mantle", and interpret the possible inconsistencies in term of superimposed mantle forces.

2. Data extraction

2.1. Choice of subduction zones

As this study focuses on the subduction process, the sampling must avoid all subduction zones perturbed by collision effects. For this reason, subduction zones with abnormal subducting plates (continental lithosphere, volcanic arc crust or oceanic lithosphere bearing oceanic plateaus) or too close to such abnormal subducting plates are systematically excluded from the sampling. All nascent subduction zones located in the compressive back-arc region of a previous and still active subduction zone are also excluded. The Flores and Wetar (behind the Timor trench), Philippine (behind the Negros subduction), Japan Sea (behind the Japan trench), Panama (behind the Costa Rica subduction) and Venezuela (behind Colombia subduction) subduction zones have thus been excluded. Likewise, the Yap, Palau, Puysegur, Sulu and North Sulawesi subduction zones have not been selected because of the shallowness of their slab (none of them pass the 250 km depth) and because of their short lateral extent (their trench lengths do not exceed 500 km). Indeed, complex asthenospheric influences are likely to perturb the dynamics of such narrow slabs (Dvorkin et al., 1993).

Finally, all the main oceanic subduction zones (70% of them are Pacific Ocean subductions, but we also include the Sunda, Manila–Negros, Ryukyu, Nankai, Antilles and Sandwich ones) have been sampled, with a sampling interval of 2° of trench, representing a total of 159 segments, and nearly 40,000 km of trench. We have preferred a uniform and systematic sampling instead of averaging data on greater segments of roughly constant subduction conditions, as done in all previous studies (1) because some single slabs exhibit such subduction conditions variability that the concept of slab segmentation could not be objectively applied (e.g., Japan–Kuril and Central America slabs); (2) to keep the possibility of analyzing the variability that some single subduction zones exhibits along their trench; and (3) to give a more accurate estimate of the variability that should occur in term of trench velocities, or back-arc deformation rates. This yields a considerably enhanced number of segment (e.g., 39 segments for Jarrard, 1986; 19 for Garfunkel et al., 1986; 27 for Otsuki, 1989) that are shown in Fig. 6. Data used in the study are listed in Table 1.

2.2. Absolute motions

To study the relative contribution of upper plate and trench motions to the overall back-arc deformation, these motions must be described in a fixed reference frame that is not attached to the plates, i.e., a terrestrial reference frame that gives each plate motion independently of mantle convection.

Several possible absolute reference frames exist, based on various assumptions. The most commonly used is the fixed hotspots reference. Among all the existing hotspots reference frames (e.g., Chase, 1978; Minster and Jordan, 1978; Gripp and Gordon, 1990), the HS3-NUVEL1A is the best constrained (see Gripp and Gordon, 2002 for discussion). The hotspot dataset HS3 consists of volcanic propagation rates and seamount segment trends from four plates. HS3-NUVEL1A, a set of angular velocities for 15 plates relative to hot spots and averaged for the last 5.7 M y^{-1}, was constructed from the HS3 data set while constraining the relative plate angular velocities to consistency with NUVEL-1A (Demets et al., 1994). No hotspots are in significant relative motion and the 95 per cent confidence is respected for all the 15 plates (the most significant uncertainties are for the slowest moving plates, i.e., Juan de Fuca, Antarctic, African and Eurasian plates).

We aim to describe, in this HS3-NUVEL1A absolute reference frame and for all the oceanic subduction zones, the motion of upper plates and trenches. The velocities are calculated at the trench, and seaward motion is defined as positive. For (main) upper plates or trenches moving away from the volcanic arc, the motion is defined as "retreat". "Advance" is used for motions directed toward the arc. For deformation rates, compression is defined as positive and extension as negative. To compare the different motions (V_{up}, V_t and V_d), we have projected them along the trench-normal azimuth (because they are a more constant feature, trenches have been preferred to volcanic arc or back-arc deformation azimuths, which are sometimes used in other studies). $V_{up(n)}$, $V_{t(n)}$ and $V_{d(n)}$, respectively, refer to the trench normal V_{up}, V_t and V_d components. Fig. 1 summarizes the different conventions.

2.2.1. Upper plate absolute motion:

HS3-NUVEL1A gives the absolute motion for all the major lithospheric plates and is sufficient to describe the motion of most subduction zones upper

Table 1
Absolute upper plate and trench motions, back-arc deformation style and rate and slab age of all oceanic subduction zones

Subduction name	Latitude (°)	Longitude (°)	Upper plate	References	$V_{up(n)}$ (mm y^{-1})	Arc-block	References	V_{tn} (mm y^{-1})	V_{dn} (mm y^{-1})	Df sup.	Age (My)
Andaman (ANDA)		92.1	Sundaland	Chamot-Rooke et al. (1997)	−19.9	Andaman Arc	Chamot-Rooke (2001)	24.4	−23.5	E3	85.5
	12	91.6	Sundaland	Chamot-Rooke et al. (1997)	−1	Andaman Arc	Chamot-Rooke (2001)	23.5	−19.7	E3	82
	10	91.4	Sundaland	Chamot-Rooke et al. (1997)	−2.1	Andaman Arc	Chamot-Rooke (2001)	15.3	−18.8	E3	77.8
	8	91.7	Sundaland	Chamot-Rooke et al. (1997)	−8.5	Andaman Arc	Chamot-Rooke (2001)	1.6	−15.1	E3	73.7
	6	92.6	Sundaland	Chamot-Rooke et al. (1997)	−8.1	Andaman Arc	Chamot-Rooke (2001)	3.9	−13.3	0	69.2
	4	93	Sundaland	Chamot-Rooke et al. (1997)	−12.6	Andaman Arc	Chamot-Rooke (2001)	−7	−4.8	0	61.1
Sumatra (SUM)	2	95	Sundaland	Chamot-Rooke et al. (1997)	−18.4	–	–	−18.4	–	0	51.8
	0	97	Sundaland	Chamot-Rooke et al. (1997)	−12.7	–	–	−12.7	–	0	46.2
	−2	98.1	Sundaland	Chamot-Rooke et al. (1997)	−14.5	–	–	−14.5	–	0	47.1
	−4	99.7	Sundaland	Chamot-Rooke et al. (1997)	−12.7	–	–	−12.7	–	0	60
	−5.5	100.8	Sundaland	Chamot-Rooke et al. (1997)	−12.3	–	–	−12.3	–	0	69
	−7	102.3	Sundaland	Chamot-Rooke et al. (1997)	−14.6	–	–	−14.6	–	0	72
Java (JAVA)	−8.4	105	Sundaland	Chamot-Rooke et al. (1997)	−14.7	–	–	−14.7	–	0	75
	−9.7	107	Sundaland	Chamot-Rooke et al. (1997)	−14.6	–	–	−14.6	–	0	78
	−10.5	109	Sundaland	Chamot-Rooke et al. (1997)	−15.7	–	–	−15.7	–	0	80
	−10.4	111	Sundaland	Chamot-Rooke et al. (1997)	−14.7	–	–	−14.7	–	0	81
	−10.7	113	Sundaland	Chamot-Rooke et al. (1997)	−14.8	–	–	−14.8	–	0	82
	−11.2	115	Sundaland	Chamot-Rooke et al. (1997)	−13.6	–	–	−13.6	–	0	83
	−11.3	117	Sundaland	Chamot-Rooke et al. (1997)	−13	–	–	−13	–	0	84
Negros (NEG)	10	121.7	Philippine Sea	Gripp and Gordon (2002)	93.6	Visayas	Rangin et al. (1999)	20.3	72.2	C3	20
Manila (MAN)	14	119.2	Philippine Sea	Gripp and Gordon (2002)	54.1	Luzon	Rangin et al. (1999)	33.5	23.9	C2	22
	16	119.2	Philippine Sea	Gripp and Gordon (2002)	54.1	Luzon	Rangin et al. (1999)	67.7	22	C2	18
	17.5	119.2	Philippine Sea	Gripp and Gordon (2002)	80.3	Luzon	Rangin et al. (1999)	81.3	–	C2	27
	19	119.8	Philippine Sea	Gripp and Gordon (2002)	95.8	Luzon	Rangin et al. (1999)	94	–	C2	32
	20.5	120.2	Philippine Sea	Gripp and Gordon (2002)	59.8	–	–	59.8	–	C1	35
Ryukyu (RYU)	23.4	124	Eurasia	Gripp and Gordon (2002)	−13.8	Ryukyu Arc	Yu and Kuo (1996), Mazzotti (1999)	30.3	−44.5	E3	35
	24.2	127	Eurasia	Gripp and Gordon (2002)	−17.5	Ryukyu Arc	Yu and Kuo (1996), Mazzotti (1999)	9	−29	E2	38
	25.7	129	Eurasia	Gripp and Gordon (2002)	−20.5	Ryukyu Arc	Yu and Kuo (1996), Mazzotti (1999)	11.8	−31.5	E2	48
	27.5	130.5	Eurasia	Gripp and Gordon (2002)	−21.1	Ryukyu Arc	Yu and Kuo (1996), Mazzotti (1999)	6.6	−29	E2	50
	29.8	132	Eurasia	Gripp and Gordon (2002)	−20.5	Ryukyu Arc	Yu and Kuo (1996), Mazzotti (1999)	9	−24.8	E2	50
Nankai (NAN)	31.8	134	Amur	Heki et al. (1999)	−9.4	–	–	−9.4	–	C1	17
	32.6	135.5	Amur	Heki et al. (1999)	−9	–	–	−9	–	C1	17
	33.1	137	Amur	Heki et al. (1999)	−8.2	–	–	−8.2	–	C1	21

Table 1 (*Continued*)

Subduction name	Latitude (°)	Longitude (°)	Upper plate	References	$V_{up(n)}$ (mm y^{-1})	Arc-block	References	V_{tn} (mm y^{-1})	V_{dn} (mm y^{-1})	Df sup.	Age (My)
Mariana (MAR)	10.8	140.5	Philippine Sea	Gripp and Gordon (2002)	−30.3	–	–	−30.3	–	E2	155
	11.4	142.5	Philippine Sea	Gripp and Gordon (2002)	−41.4	–	–	−41.4	–	E3	155
	12	144.5	Philippine Sea	Gripp and Gordon (2002)	−58	Mariana Arc	Martinez et al. (2000)	−25.3	−33.3	E3	156
	13.3	146.5	Philippine Sea	Gripp and Gordon (2002)	−75.8	Mariana Arc	Martinez et al. (2000)	−37.3	−38	E3	156.3
	15	147.5	Philippine Sea	Gripp and Gordon (2002)	−83.7	Mariana Arc	Martinez et al. (2000)	−49.9	−34.4	E3	153.2
	17	147.8	Philippine Sea	Gripp and Gordon (2002)	−76.9	Mariana Arc	Martinez et al. (2000)	−43.3	−35.3	E3	149.6
	19	147.6	Philippine Sea	Gripp and Gordon (2002)	−69.8	Mariana Arc	Martinez et al. (2000)	−37.5	−32	E3	147.5
	21	146.9	Philippine Sea	Gripp and Gordon (2002)	−45.6	Mariana Arc	Martinez et al. (2000)	−29.6	−14.8	E3	146.6
	23	145.1	Philippine Sea	Gripp and Gordon (2002)	−31.4	Mariana Arc	Martinez et al. (2000)	−27.3	−2.8	E3	145.3
Izu−Bonin (IZU)	27	143.3	Philippine Sea	Gripp and Gordon (2002)	−60.7	–	–	−60.7	–	E2	148
	29	142.9	Philippine Sea	Gripp and Gordon (2002)	−45.6	–	–	−45.6	–	E2	141
	31	142.3	Philippine Sea	Gripp and Gordon (2002)	−45.9	–	–	−45.9	–	E2	135
	33	142.1	Philippine Sea	Gripp and Gordon (2002)	−44.1	–	–	−44.1	–	E2	129
Japan (JAP)	35	142.2	Amur	Heki et al. (1999)	−11.9	Honshu	Mazzotti et al. (2001)	−21.2	7.7	C3	127
	37	143.5	Amur	Heki et al. (1999)	−11.9	Honshu	Mazzotti et al. (2001)	−20	8.7	C3	132
	39	144.2	Amur	Heki et al. (1999)	−10.7	Honshu	Mazzotti et al. (2001)	−20	9.6	C3	131
	40.5	144.5	Amur	Heki et al. (1999)	−11	Honshu	Mazzotti et al. (2001)	−19.6	8.6	C3	128
Kuril (KUR)	41.5	145.5	North America	Gripp and Gordon (2002)	−23.3	–	–	−23.3	–	C2	128
	42.2	147	North America	Gripp and Gordon (2002)	−21.9	–	–	−21.9	–	C2	120
	43.5	149	North America	Gripp and Gordon (2002)	−22.3	–	–	−22.3	–	C2	118
	44.4	151	North America	Gripp and Gordon (2002)	−18.8	–	–	−18.8	–	C2	118
	45.3	153	North America	Gripp and Gordon (2002)	−20.7	–	–	−20.7	–	C2	118
	47	155.1	North America	Gripp and Gordon (2002)	−21.7	–	–	−21.7	–	C1	110
	49	157.5	North America	Gripp and Gordon (2002)	−18.9	–	–	−18.9	–	C1	110
	51	160.2	North America	Gripp and Gordon (2002)	−19.2	–	–	−19.2	–	C1	110
Kamchatka (KAM)	53	162.3	North America	Gripp and Gordon (2002)	−17.7	–	–	−17.7	–	E1	100
	54.5	163.6	North America	Gripp and Gordon (2002)	−16.7	–	–	−16.7	–	E1	100
Aleutian (ALE)	51.6	173	North America	Gripp and Gordon (2002)	4.6	–	–	4.6	–	0	45
	51.1	175	North America	Gripp and Gordon (2002)	1.6	–	–	1.6	–	0	45
	50.8	177	North America	Gripp and Gordon (2002)	−3.4	–	–	−3.4	–	C1	54
	50.4	179	North America	Gripp and Gordon (2002)	−0.8	–	–	−0.8	–	C1	56
	50.3	181	North America	Gripp and Gordon (2002)	−1.6	–	–	−1.6	–	0	58
	50.4	183	North America	Gripp and Gordon (2002)	−5	–	–	−5	–	0	58
	50.5	185	North America	Gripp and Gordon (2002)	−4.6	–	–	−4.6	–	0	58
	50.9	187	North America	Gripp and Gordon (2002)	−3.3	–	–	−3.3	–	0	63
	51.1	189	North America	Gripp and Gordon (2002)	−6	–	–	−6	–	0	63
	51.5	191	North America	Gripp and Gordon (2002)	−7.3	–	–	−7.3	–	0	61
	52	193	North America	Gripp and Gordon (2002)	−6	–	–	−6	–	E1	59
	52.5	195	North America	Gripp and Gordon (2002)	−5.7	–	–	−5.7	–	E1	58
	53.1	197	North America	Gripp and Gordon (2002)	−4.8	–	–	−4.8	–	0	53

Alaska (ALA)	53.5	199	North America	Gripp and Gordon (2002)	−3.7	–	–	−3.7	–	0	52
	53.8	201	North America	Gripp and Gordon (2002)	−3.2	–	–	−3.2	–	0	52
	54.2	203	North America	Gripp and Gordon (2002)	−3	–	–	−3	–	0	52
	54.8	205	North America	Gripp and Gordon (2002)	−7	–	–	−7	–	0	52
	55.6	207	North America	Gripp and Gordon (2002)	−4.5	–	–	−4.5	–	0	49
	56.2	209	North America	Gripp and Gordon (2002)	−4.1	–	–	−4.1	–	C1	46
	57.1	211	North America	Gripp and Gordon (2002)	−6.2	–	–	−6.2	–	C1	45
	58	213	North America	Gripp and Gordon (2002)	−6.4	–	–	−6.4	–	C1	40
	59.1	214.5	North America	Gripp and Gordon (2002)	−6.8	–	–	−6.8	–	C1	39
	59.2	215.5	North America	Gripp and Gordon (2002)	1.5	–	–	1.5	–	C1	39
Cascadia (CASC)	50	231.7	North America	Gripp and Gordon (2002)	21	–	–	18.8	–	0	5
	48	233.4	North America	Gripp and Gordon (2002)	22	–	–	19.7	–	0	10
	46	234.1	North America	Gripp and Gordon (2002)	23.8	–	–	22.8	–	0	11
	44	234.6	North America	Gripp and Gordon (2002)	24	–	–	24	–	0	11
	42	234.7	North America	Gripp and Gordon (2002)	25.3	–	–	23.9	–	E1	10
Mexico (MEX)	19.1	254.5	North America	Gripp and Gordon (2002)	35.7	–	–	35.7	–	E1	8
	17.9	256	North America	Gripp and Gordon (2002)	29.7	–	–	29.7	–	E1	8
	16.9	258	North America	Gripp and Gordon (2002)	25.1	–	–	25.1	–	E1	15
	16.3	260	North America	Gripp and Gordon (2002)	23.2	–	–	23.2	–	E1	15
	15.6	262	North America	Gripp and Gordon (2002)	21.7	–	–	21.7	–	E1	15
	15.3	264	North America	Gripp and Gordon (2002)	16.7	–	–	16.7	–	E1	15
Costa-Rica (COST)	14.2	266	Caribbean	Gripp and Gordon (2002)	21.4	–	–	21.4	–	E1	18
	13.2	268	Caribbean	Gripp and Gordon (2002)	19.6	–	–	19.6	–	0	22
	12.3	270	Caribbean	Gripp and Gordon (2002)	18.5	–	–	18.5	–	0	24
	11.4	272	Caribbean	Gripp and Gordon (2002)	22.3	–	–	22.3	–	0	28
	9.4	274	Caribbean	Gripp and Gordon (2002)	21.6	–	–	21.6	–	C1	26
Colombia (COL)	5	281.9	South America	Gripp and Gordon (2002)	38.6	North Andean Block	Freymuller et al. (1993)	27.4	8	C3	19
	3.5	280.9	South America	Gripp and Gordon (2002)	35.9	North Andean Block	Freymuller et al. (1993)	33	2.5	C3	15
	2	279.9	South America	Gripp and Gordon (2002)	38.2	North Andean Block	Freymuller et al. (1993)	25.2	12.7	C3	12
Peru (PER)	−4	278.1	South America	Gripp and Gordon (2002)	46.6	–	–	46.6	–	C3	30
	−5.5	278.1	South America	Gripp and Gordon (2002)	47	–	–	47	–	C3	30
	−7	278.4	South America	Gripp and Gordon (2002)	45.9	–	–	45.9	–	C3	31
	−9	279.2	South America	Gripp and Gordon (2002)	45.1	–	–	45.1	–	C3	31
	−11	280.4	South America	Gripp and Gordon (2002)	43.8	–	–	43.8	–	C3	46
	−13	281.7	South America	Gripp and Gordon (2002)	42.6	–	–	42.6	–	C3	46
North Chile (NCHI)	−17	285.9	South America	Gripp and Gordon (2002)	34.4	–	–	34.4	–	C3	52
	−19	288	South America	Gripp and Gordon (2002)	43.6	Andes	Klotz et al. (2001)	34.6	9.3	C3	54
	−21	288.7	South America	Gripp and Gordon (2002)	47.9	Andes	Klotz et al. (2001)	41.9	6	C3	55
	−23	288.7	South America	Gripp and Gordon (2002)	46.6	Andes	Klotz et al. (2001)	41.8	4.7	C3	54
	−25	288.6	South America	Gripp and Gordon (2002)	46.9	Andes	Klotz et al. (2001)	41	5.8	C3	53
	−27	288.3	South America	Gripp and Gordon (2002)	45.1	Andes	Klotz et al. (2001)	39.4	5.5	C3	52
Juan Fernandez (JUAN)	−29	287.7	South America	Gripp and Gordon (2002)	44.6	Andes	Klotz et al. (2001)	38.9	5.2	C3	49
	−32	287.4	South America	Gripp and Gordon (2002)	45.7	Andes	Klotz et al. (2001)	38.8	5.2	C3	48

Table 1 (*Continued*)

Subduction name	Latitude (°)	Longitude (°)	Upper plate	References	$V_{up(n)}$ (mm y^{-1})	Arc-block	References	V_{tn} (mm y^{-1})	V_{dn} (mm y^{-1})	Df sup.	Age (My)
South Chile (SCHI)	−34	286.9	South America	Gripp and Gordon (2002)	38.9	–	–	38.9	–	C1	42
	−35.5	286.2	South America	Gripp and Gordon (2002)	36.5	–	–	36.5	–	C1	39
	−37	285.4	South America	Gripp and Gordon (2002)	42	–	–	42	–	C1	35
	−39	284.9	South America	Gripp and Gordon (2002)	43	–	–	43	–	C1	33
	−41	284.7	South America	Gripp and Gordon (2002)	43.3	–	–	43.3	–	C1	20
Chile triple junction (TRI)	−43	284.5	South America	Gripp and Gordon (2002)	42.7	–	–	42.7	–	0	12
	−45	283.9	South America	Gripp and Gordon (2002)	41.7	–	–	41.7	–	0	5
	−47	283.8	South America	Gripp and Gordon (2002)	40.2	–	–	40.2	–	0	10
	−49	282.6	South America	Gripp and Gordon (2002)	40.8	–	–	40.8	–	0	18
Patagonia (PAT)	−51	283.3	South America	Gripp and Gordon (2002)	41	–	–	41	–	0	18
	−53	283.9	South America	Gripp and Gordon (2002)	39.6	–	–	39.6	–	0	20
	−55	286.7	South America	Gripp and Gordon (2002)	32.3	–	–	32.3	–	0	20
Antilles (ANT)	12	302.6	Caribbean	Gripp and Gordon (2002)	−28.1	–	–	−28.1	–	E1	117
	14	302.3	Caribbean	Gripp and Gordon (2002)	−29.8	–	–	−29.8	–	E1	110
	16	301.2	Caribbean	Gripp and Gordon (2002)	−31	–	–	−31	–	E1	98
	18	299.8	Caribbean	Gripp and Gordon (2002)	−27.6	–	–	−27.6	–	E1	90
	19.3	298	Caribbean	Gripp and Gordon (2002)	−30.5	–	–	−30.5	–	E1	84
	19.8	296	Caribbean	Gripp and Gordon (2002)	−11.7	–	–	−6.6	−4.9	E1	92
	19.8	294	Caribbean	Gripp and Gordon (2002)	−7.3	–	–	−1.3	−4.1	E1	100
	19.7	292	Caribbean	Gripp and Gordon (2002)	−7.3	–	–	−1.3	−4	E1	110
Sandwich (SAND)	−60	335.4	Scotia	Gripp and Gordon (2002)	−15.7	Sandwich Islands	Vanneste et al. (2002)	17.9	−33.7	E3	33
	−58	336.2	Scotia	Gripp and Gordon (2002)	−24.4	Sandwich Islands	Vanneste et al. (2002)	49	−72.8	E3	36
	−56	334.9	Scotia	Gripp and Gordon (2002)	−26.9	Sandwich Islands	Vanneste et al. (2002)	39.4	−62.1	E3	40
	−55.1	333	Scotia	Gripp and Gordon (2002)	−20.8	Sandwich Islands	Vanneste et al. (2002)	8.5	−28.8	E3	40
	−54.9	331	Scotia	Gripp and Gordon (2002)	−13.2	Sandwich Islands	Vanneste et al. (2002)	−1.9	−10.1	E3	40
	−54.8	329	Scotia	Gripp and Gordon (2002)	−15.8	Sandwich Islands	Vanneste et al. (2002)	−17	–	E1	40
Kermadec (KER)	−35	181.6	Australia	Gripp and Gordon (2002)	−53.7	–	–	−53.7	–	E2	95
	−33	182.2	Australia	Gripp and Gordon (2002)	−49	–	–	−49	–	E2	97
	−31	183.2	Australia	Gripp and Gordon (2002)	−49.8	–	–	−49.8	–	E2	99
	−29	183.9	Australia	Gripp and Gordon (2002)	−44.9	–	–	−44.9	–	E2	101
	−27	184.5	Australia	Gripp and Gordon (2002)	−39.4	–	–	−39.4	–	E2	103
Tonga (TONG)	−23	185.4	Australia	Gripp and Gordon (2002)	−47	Tonga Arc	Pelletier et al. (1998)	−8	−39.2	E3	106
	−21	186.5	Australia	Gripp and Gordon (2002)	−40.4	Tonga Arc	Pelletier et al. (1998), Zellmer and Taylor (2001)	40.4	−76	E3	107
	−19	187.2	Australia	Gripp and Gordon (2002)	−35.2	Tonga Arc	Pelletier et al. (1998), Zellmer and Taylor (2001)	93	−106.9	E3	108

	−17	187.8	Australia	Gripp and Gordon (2002)	−35.2	Tonga Arc	Pelletier et al. (1998), Zellmer and Taylor (2001)	93	−106.9	E3	108
	−15.5	187.7	Australia	Gripp and Gordon (2002)	−28	Tonga Arc	Pelletier et al. (1998), Zellmer and Taylor (2001)	113.6	−142.1	E3	109
New Hebrides (NHEB)	−20	168.2	Pacific	Gripp and Gordon (2002)	56.6	New Hebrides Arc	Pelletier et al. (1998), Zellmer and Taylor (2001)	101	−45.5	E3	45
	−18	167.4	Pacific	Gripp and Gordon (2002)	85.4	New Hebrides Arc	Pelletier et al. (1998), Zellmer and Taylor (2001)	96.1	−3.3	E3	48
	−14	166.2	Pacific	Gripp and Gordon (2002)	90.6	New Hebrides Arc	Pelletier et al. (1998), Zellmer and Taylor (2001)	105.1	−15.6	E3	60
	−12	165.7	Pacific	Gripp and Gordon (2002)	67.4	New Hebrides Arc	Pelletier et al. (1998), Zellmer and Taylor (2001)	144.7	−75.2	E3	
New Britain (NBRIT)	−6.1	152	North Bismarck	Tregoning (2002)	−90.4	South Bismarck	Tregoning et al. (1998, 1999)	19.5	−109.1	E3	31
	−7	150	North Bismarck	Tregoning (2002)	−94.4	South Bismarck	Tregoning et al. (1998, 1999)	−17.5	−73.6	E3	31
	−7.3	148	North Bismarck	Tregoning (2002)	0	South Bismarck	Tregoning et al. (1998, 1999)	−22	−16.6	E3	31

For each segment, we give: the subduction name with its associated abbreviation, the geographic coordinates of the trench in the middle of the segment; latitude positive northward; longitude from 0 to 360°, the upper plate name, the reference used for its absolute motion estimate and its trench-normal component ($V_{\mathrm{up(n)}}$), the associated "arc-block" name, the reference used for its absolute motion estimate and the normal-to-the-trench component of trench absolute motion ($V_{\mathrm{t(n)}}$), the normal-to-the-trench component of back-arc deformation rate ($V_{\mathrm{d(n)}}$) and the associated strain regime class (Df class), the age of the subducting lithosphere, estimated from Müller et al., 1997.

plates. Nevertheless, the accuracy can be improved for several subduction zones, introducing some other plates or micro-plates, whose motion is known from independent GPS data: the Sundaland block (Chamot-Rooke et al., 1997), the Amurian plate (Heki et al., 1999) and the North-Bismarck plate (Tregoning, 2002). These plates and micro-plates are shown in Fig. 6.

2.2.2. *Trench absolute motion:*

The existence of back-arc deformation implies the development, in the upper plate and near the plate boundary, of a new structural element, here called "arc" (Fig. 1), that has its own motion (Fig. 6 and Table 1 show the different "arc-blocks" used in this study). The arc absolute motion ($V_{\rm arc}$) can be calculated from upper plate absolute motion and back-arc deformation rate (Carlson and Melia, 1984). If we assume negligible tectonic accretion and erosion rates – they are generally estimated to be less than 10 mm y^{-1} (Lallemand, 1995) – the arc could be considered as interdependent with the subduction hinge and its motion also gives trench migration ($V_{\rm t} = V_{\rm arc}$). Accurate $V_{\rm d}$ estimates are mainly given by GPS data, or calculated from magnetic isochrons in some cases (see Table 1 for the used references). They are available for all the fastest deforming regions (e.g., Tonga, Mariana and Chile). In subduction zones where diffuse back-arc deformation occurs, the arc is interdependent with the upper plate. Upper plate absolute motion then gives a good approximation of trench migration ($V_{\rm t} = V_{\rm up}$).

2.3. *Back-arc deformation style*

Ideally, the continuum of possible back-arc deformation style, from highly extensional to highly compressive, is given by the deformation rate. However, those data are not available with enough accuracy for all subduction zones, especially for the lowest deformation rates. To include a maximum of subduction zones in the study, following the approach of Jarrard (1986), the strain regime of all oceanic subduction zones is estimated in a semi-quantitative way from dominant focal mechanisms of earthquakes occurring within the upper-plate: each subduction zone is classified into a continuum of seven strain classes (Fig. 7b), from highly extensional (class E3, back-arc spreading) to highly compressive (class C3, back-arc shortening).

From class E3 to class E1, strike-slip focal mechanisms become more and more dominant over normal mechanisms, and the strain becomes less and less extensive. Class 0, is characterized by dominant strike-slip focal mechanisms or almost neutral stress fields (no earthquakes occurring within the upper plate). From class C1 to C3, compressive focal mechanisms become more and more dominant over strike-slip events, and the strain more and more compressive. Additional criteria are taken into account to characterize the two end-member cases: back-arc spreading occurs for all subduction zones of class E3 (whereas subduction zones of class E2 are only in a rifting stage) and all subduction zones of class C3 generate lithospheric scale back-arc thrusting.

Focal mechanisms of earthquakes occurring within the upper plate are extracted from all the earthquakes occurring between 0 and 40 km depth recorded in the online Harvard Seismology catalog. Among these earthquakes, only those occurring within upper plates are extracted: the aim is for the selection to approach the trench as nearly as possible, while avoiding the compressive subduction earthquakes near the interplate interface. For this (Fig. 7a), using trench-normal cross sections of the seismic slab (hypocenters are from the relocated earthquakes catalog EHB98 of Engdahl et al., 1998), the distance to the trench for which the slab crosses the 60 km isodepth contour (D_{60}) is determined. Then, all the focal mechanisms located at a minimal distance D_{60} from the trench are extracted. As the extraction box is parallel to the trench, a rigorous selection can only be applied to trench segments, which are nearly linear. Trenches are thus broken up in as many segments as necessary.

2.4. *Slab age*

The digital age grid of Müller et al. (1997) gives the age of the main world's ocean floor with a node interval of 6 arcmin. The age of each grid node is determined by linear interpolation between adjacent isochrons (given by magnetic anomalies) in the spreading direction. The resulting accuracy of the age grid has been calculated to be generally smaller than 1 My.

For most of the segments, slab age at the trench is estimated from this age grid, averaging the subducting plate age on the first 10 km from the trench, in a trench-normal direction. However, because of long

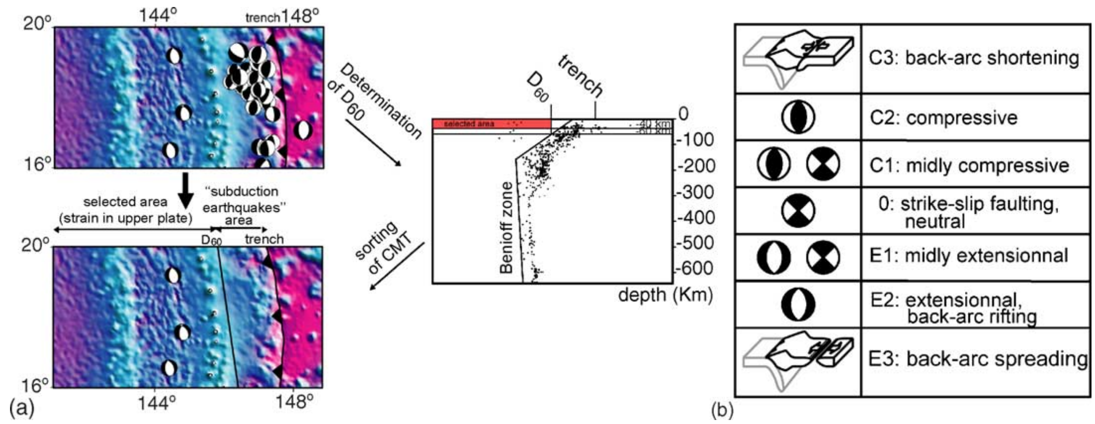

Fig. 7. (a) Selection of focal mechanisms of earthquakes occurring within the upper plate: among earthquakes occurring between 0 and 40 km depth (Harvard Seismology catalog), all the focal mechanisms located at a minimum distance, D_{60}, of the trench are extracted (D_{60} = distance from trench to point at which the slab crosses the 60 km isodepth contour), allowing the selection of earthquakes occurring within the upper plate while avoiding the compressive subduction earthquakes near the plate interface. (b) Back-arc strain regime classification.

time intervals without changes in the Earth's magnetic field (such as the Cretaceous Quiet Zone from 118 to 83 My), plate ages in several zones remain partly defined by the age grid. This lack of data is significant for

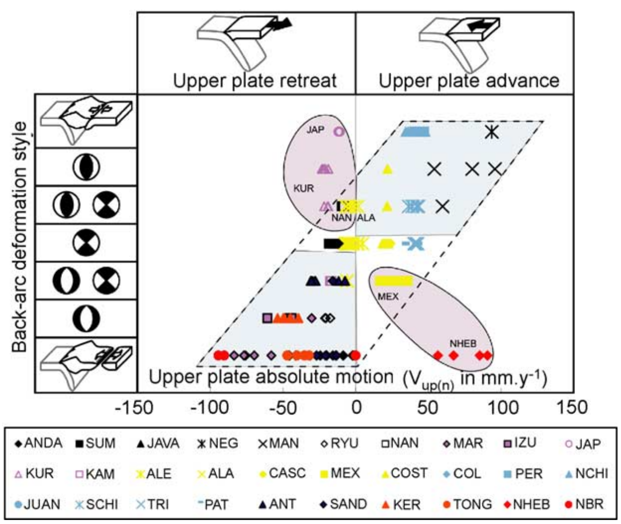

Fig. 8. Cross-plot of back-arc deformation style versus trench-normal component of upper plate absolute motion ($V_{up(n)}$). Blue area: subduction zones that have back-arc deformation style consistent with upper plate absolute motion (correspondence between back-arc extension and upper plate retreat and between back-arc compression and upper plate advance). Red area: back-arc deformation style inconsistent with upper plate absolute motion. The dashed line delimits the global trend, that is increasing extension with increasing upper plate retreat and conversely for compression.

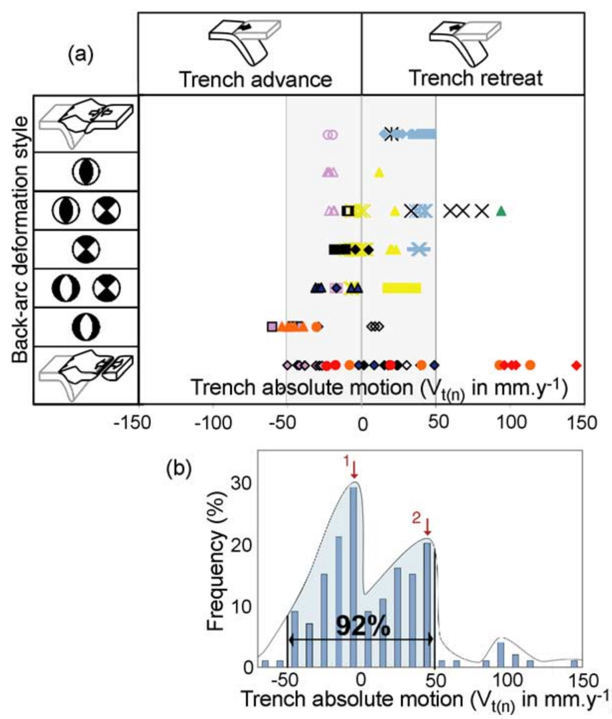

Fig. 9. (a) Cross-plot of back-arc deformation style versus normal-to-the-trench component of trench absolute motion ($V_{t(n)}$). See Fig. 8 and Table 1 for subduction zone symbols and abbreviations. (b) $V_{t(n)}$ frequency diagram: 92% of the trenches get $V_{t(n)}$ limited to ± 50 mm y^{-1}. Two main populations are identified: population (1) which is more or less centered on the 0 value and population (2) which exhibits significant trench retreat.

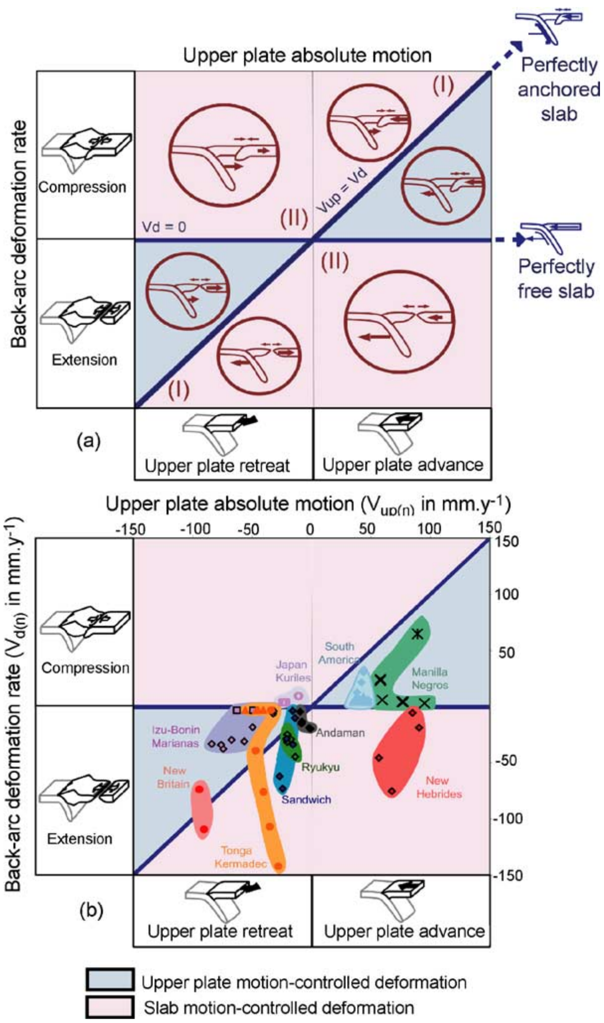

Fig. 10. Quantitative examination of the upper plate absolute motion effect. (a) Theoretical slab/trench behavior as a function of subduction position in $V_{d(n)}/V_{up(n)}$ space. Subduction zones position with respect to two reference lines, the “perfectly anchored slab” line ($V_{d(n)} = V_{up(n)}$) and the “perfectly free slab” line ($V_{d(n)} = 0$), is analyzed in $V_{d(n)}$ versus $V_{up(n)}$ cross-plot. The reference lines delimit the subduction zones that have “upper plate motion-controlled deformation” (slab/trench more or less follows the upper plate absolute motion) from those that get “slab motion-controlled deformation” (slab/trench has its own motion, at least partly independent of upper plate absolute motion). Slab/trench independent motion can generate (I) excess of deformation relative to rate allowed by a single $V_{up(n)}$ influence or (II) deformation style opposite to those expected with the direction of upper plate absolute motion relatively to the trench. (b) Cross-plot of trench-normal component of back-arc deformation rate ($V_{d(n)}$) versus trench-normal component of upper plate absolute motion ($V_{up(n)}$), see Fig. 8 for symbols.

our study: Cretaceous was the time of plate formation for most of the segments of the Western Pacific subduction zones (Tonga–Kermadec, Izu-Bonin–Mariana and Japan–Kuril). For these segments, slab age at the trench is manually extrapolated from the nearest magnetic anomaly. For the small basins that are subducted in the New Hebrides and New Britain zones, not included in the Müller et al. (1997) age grid, ages are taken from Jolivet (1995).

3. Data analysis

3.1. $V_{up(n)}$ or $V_{t(n)}$ dominant control on back-arc deformation style?

The purpose of this section is to test whether or not one of the two boundary plate motions (V_{up} and V_t) exerts a dominant control on the observed strain regime. Figs. 8 and 9, respectively, show the relations between the back-arc deformation style, as defined in Section 2.3, and V_{up} trench-normal component ($V_{up(n)}$), and between this back-arc deformation style and trench-normal component of trench absolute motion ($V_{t(n)}$).

3.1.1. Back-arc deformation style relation with $V_{up(n)}$ (Fig. 8)

If we exclude neutral subduction (class 0), 75% of oceanic subduction zones show a good correspondence between upper plate absolute motion with respect to the trench and the back-arc deformation style: retreating upper plates are preferentially associated with back-arc extension (class E1–E3) and advancing ones with back-arc compression (class C1–C3). The global trend

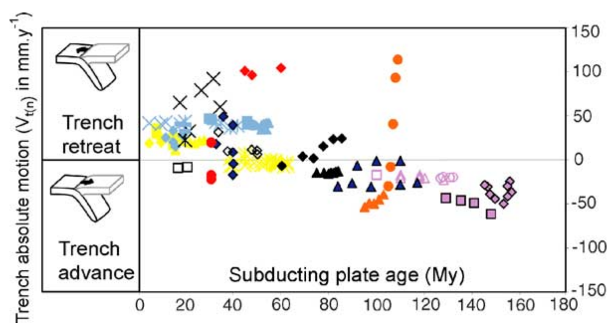

Fig. 11. Cross-plot of trench-normal component of trench absolute motion ($V_{t(n)}$) versus slab age, see Fig. 8 for symbols.

indicates the most intense deformations occur for the fastest moving upper plates.

This correlation is strong, even if the upper plate deformation for 25% of subduction zones is inconsistent with the global trend. All the exceptions are more or less questionable cases. The most striking case of non-correlation is New Hebrides, which associates an active back-arc spreading in the North Fiji Basin with a fast advancing Pacific plate (nearly 100 mm y^{-1}), but the plate configuration in the New Hebrides region may be too complex to reliably pick a single major upper plate in the system (Pelletier et al., 1998). The Japan–Kuril subduction, with its strong back-arc compression (class C1–C3) associated with upper plate retreat, is also an exceptional case but inconsistencies may come from uncertainties in the tectonic setting of Eastern Asia (Miyasaki et al., 2001) and from the upper plate retreat slowness (20 mm y^{-1} at the most), which may reach the reference frame accuracy limits. Similarly, there are a few exceptions (Mexico, Cascadia, Nankai and Alaska), which imply slow $V_{up(n)}$ (25 mm y^{-1} at the most) and diffuse deformations (class E1 and C1) in a sense opposite to those globally followed.

Even if 75% of subduction zones verify the global trend, the correlation is not perfect: some subduction zones are on the fringe of the tendency, showing low deformations for fast moving upper plates (e.g., Izu-Bonin, with a low extension (E2) associated with a fast Philippine Sea plate retreat of about 50 mm y^{-1}, or the Manila–Negros subduction, with a low compression (C2) despite a nearly 90 mm y^{-1} Philippine Sea plate advance) or conversely, high deformations for slowly moving upper plates (e.g., Andaman, Scotia or Ryukyu subductions, where back-arc spreading is associated with upper plate retreat that reaches 20 mm y^{-1} at the most). On a more local scale, the only lateral changes in upper plate absolute motion often fails to explain the back-arc strain regime variability that occurs along some plate boundaries. For example, the variations of extension observed along the Tonga–Kermadec plate boundary show an opposite than expected relation to lateral changes in Australian plate absolute motion, i.e., from Tonga to Kermadec extension intensity decreases from class E3 to class E1 while absolute motion of the Australian plate retreat shows a gradual increase from 30 to 50 mm y^{-1}. Additional influences should thus certainly act with $V_{up(n)}$ to account for the overall deformation variability.

3.1.2. Back-arc deformation style relation with $V_{t(n)}$ (Fig. 9)

No clear relation appears between trench motion and back-arc deformation mode (Fig. 9a): back-arc extension and compression occur equally for trench retreat or advance. Likewise, no preferential trench-relative direction is identified: there are almost as many retreating trenches (52%) as advancing ones (48%).

The frequency diagram of $V_{t(n)}$, which shows a majority of trench migrations more or less centered on the 0 value (population 1, Fig. 9b), is consistent with an anchoring effect. However, the large number of subduction zones with significant trench retreat (population 2, Fig. 9b), attests to the influence of a secondary driving mechanism that favors trench rollback. In any case, the most striking feature of the histogram is the limitation, for 92% of the trenches, of $V_{t(n)}$ to ± 50 mm y^{-1}. The few exceptions occur mainly for seaward trench migration and concern segments from subduction zones associated with back-arc spreading (Tonga and New Hebrides) and from the Manila–Negros subduction.

3.2. Quantitative examination of the $V_{up(n)}$ influence (Fig. 10)

From Section 3.1, we conclude that upper plate absolute motion appears to exert a dominant control on back-arc deformation, relative to the influence of trench absolute motion. Resistance to slab migration is thus needed to more or less inhibit the trench from following upper plate motion and to explain the observed deformation. Theoretically, anchoring, but also slab pull and mantle flow induced forces are likely to provide such resistance. Their respective effects cannot be directly determined, but a quantitative examination of the $V_{up(n)}$ influence may provide some information.

As seen in Section 1.2, the anchoring-force (see Fig. 3) results from a passive and viscous mantle resistance to slab migration, making upper plate absolute motion the major cause of back-arc deformation. As a consequence, a single anchoring effect implies that for a given upper plate absolute motion, the back-arc deformation rate is a function of the anchoring-force efficiency, i.e., the more efficient this force is, the higher $V_{d(n)}$ should be – and that back-arc deformation rates cannot exceed the $V_{up(n)}$ value. For fully efficient anchoring-force, the slab is perfectly anchored and $V_{d(n)}$ reaches the $V_{up(n)}$ limit value. Conversely, for totally inefficient anchoring-force ("perfectly free slabs"), the slab strictly follows the upper plate motion and no back-arc deformation occurs.

As Otsuki did in 1989, these two end-member cases ("perfectly free slabs" and "perfectly anchored slabs") can be used as references to test, in a cross-plot of $V_{up(n)}$ versus $V_{d(n)}$ (Fig. 10), wheither a single anchoring-force influence can account for all the observed deformations or if additional mechanisms are needed. The position of all subduction zones is analyzed relative to the two corresponding reference lines, i.e., "perfectly anchored slabs" line ($V_{d(n)} = V_{up(n)}$) and "perfectly free slabs" line ($V_{d(n)} = 0$), which delimit two main fields (Fig. 10a). Between the lines is the "upper plate motion-controlled deformation field", where back-arc deformation could be explained by a global resistive force, i.e., a combination of anchoring, slab pull and mantle flow induced forces that inhibits the slab from following upper plate motion. The total resistance increases from the "perfectly free slabs" line toward the "perfectly anchored slabs" line.

Outside the lines is the "slab motion-controlled deformation field", for which $V_{up(n)}$ can not account for all the observed deformation; either there is an excess of deformation relative to the maximum rate allowed by the anchoring effect ($V_{d(n)} > V_{up(n)}$), or the back-arc deformation style is opposite to that predicted by $V_{up(n)}$. A mechanism in addition to a single passive anchoring effect must act on slabs to explain the observed $V_{d(n)}$: slabs migrate at least partly independently from the upper plate motion, indicating that another force is active, i.e., slab pull and/or mantle flow associated forces.

Fig. 10b shows the cross-plot of $V_{up(n)}$ versus $V_{d(n)}$ for all subductions of well-characterized back-arc deformation (a total of 80 segments including class E3 and E2 for extension and class C3 and C2 for compression, for which accurate back-arc deformation rates data are available).

Almost 60% of the analyzed segments fall inside the "upper plate motion-controlled deformation field". This is mostly verified for 4/5 of the subduction zones associated with back-arc compression, whereas it includes only half of the segments associated with back-arc extension. "Perfectly anchored slabs" are rarely observed, whereas almost 45% of the "upper plate motion-controlled deformation field" subductions are located near the "perfectly free slabs" line. We observe that a number of those "perfectly free slabs" associate low back-arc deformation rates with fast moving upper plates (e.g., Manila, Izu-Bonin and Kermadec).

The remaining 40%, which are mostly represented by segments of back-arc spreading associated subductions (all these subductions are represented except for Mariana), get "slab motion-controlled deformation". Most of them, including Tonga, Sandwich, Ryukyu and also Andaman and New Britain, to a lesser extent, exhibit "excess deformation" with respect to the "available" upper plate velocity. These subductions are not undergoing excess deformation along their entire length: instead, along strike they change from the "upper plate-controlled deformation field" to cross over the "perfectly anchored slabs" line somewhere along their lengths. As seen in Section 3.1.1, the New Hebrides and Japan–Kuril subductions have deformation opposite that predicted by the global trend between strain regime and upper plate absolute motion.

3.3. $V_{t(n)}$ and slab age relation: slab pull effect on trench motion?

We have seen above that there are as many retreating trenches as advancing ones. This observation opens to question the validity of the assumption that attributes trench motion to slab pull. However, we have also seen that 40% of the studied cases fall into the "slab motion-controlled deformation" field. By definition, the upper plate motion cannot explain such back-arc deformations, implying the existence, at least in these particular subduction zones, of an additional driving mechanism for both back-arc deformation and trench motion. The "slab rollback model", which assumes that the older and colder a slab is, the harder it should pull down on the hinge and the faster it should rollback, is one of the most widely diffused ideas in the geological literature. The efficiency of such a spontaneous rollback is easily testable from our data.

Fig. 11 shows a cross-plot of $V_{t(n)}$ versus slab age for the 159 sampled segments. No correlation of increasing trench rollback with increasing slab age is clear among current subduction zones. In fact, the apparent trend is for faster rollback with younger slabs, i.e., the opposite of the trend predicted by the theoretical rule. As a consequence, most of the subduction zones associated with the oldest slabs have advancing trenches instead of the fast rollback that slab pull influence predicts.

4. Discussion

Among the two boundary plate motions imposed on arc/back-arc systems (V_{up} and V_t), upper plate absolute motion appears to exert a dominant control on back-arc deformation, relative to trench absolute motion influence. The observed correlation (Fig. 8) is in good agreement with many earlier observations (e.g., Hyndman, 1972; Chase, 1978; Jarrard, 1986). Statistical analysis by Jarrard (1986), which has previously shown that among a set of 26 parameters, upper plate absolute motion is the best single predictor of back-arc deformation style, confirms V_{up} as a first order parameter in the control of back-arc strain regime.

To explain the observed deformations, resistance to slab migration is needed to more or less inhibit the trench from following upper plate motion. Not only anchoring, but also slab pull and mantle flow-induced forces are likely to provide such resistance. However, the observed correlation implies a dominant upper plate motion-induced resistance that is an anchoring effect (see Fig. 3), even if slab pull and mantle flow influences can not rigorously be eliminated. The importance of this anchoring force in subduction dynamics has been emphasized by Scholz and Campos (1995) who have estimated it for 29 circum-pacific subduction zones and found that it successfully predicts most of back-arc spreading occurrence (80%).

However, the fact that trenches are not statistically stationary – many advancing and retreating trenches have been recognized in this study and in earlier ones (e.g., Carlson and Melia, 1984; Jarrard, 1986; Garfunkel et al., 1986; Carlson and Mortera-Gutiérrez, 1990) – can not easily be reconciled with the idea of slabs perfectly anchored in their surrounding mantle. We must be aware from Fig. 8 that perfect anchoring is rarely observed. This feature poses the problem of the anchoring force efficiency, for which a global approximation may be given by the general $V_{t(n)}$ limitation to $\pm 50\,\mathrm{mm\,y^{-1}}$ (Fig. 9), indicating that, at best, slabs are only partly anchored.

The low magnitude of the anchoring force is particularly indicated by the large number of subduction zones that have almost "perfectly free slabs", and especially by those that associate low back-arc deformation rates with fast moving upper plates—e.g., Izu-Bonin, Manila, Kermadec (Fig. 10b), implying that trenches are often driven solely by the upper plate motion. It thus seems that the anchoring-force may sometimes be insufficient to counteract the efficiency of the upper plate-trench coupling. As suggested by Carlson and Mortera-Gutiérrez (1990) in order to explain the Izu-Bonin-Mariana trench advance, we think that upper plate motion generates an excess of pressure on the plate interface and possibly in the asthenospheric wedge overlying the slab. Such pressure would act along the top surface of the slab, making the trench interdependent from the upper plate, which would then tend to drive the subduction hinge and generating slab dip change and/or forward/backward migration (Fig. 3).

Despite the global control of upper plate absolute motion on back-arc deformation style, "slab motion-controlled" deformations exist. All the subduction zones associated with back-arc spreading are concerned except for the Marianas, whereas "upper plate motion-control" is sufficient to explain most of compressive back-arc deformations. A mechanism in addition to a single anchoring effect, i.e., slab pull or mantle flows – is thus needed to explain deformation rates and trench rollback observed in back-arc spreading associated-subductions. Evidence of a secondary driving mechanism which favors trench rollback is supported by the $V_{t(n)}$ distribution (Fig. 9b).

There are two reasons for ruling out the idea of a spontaneous trench rollback related to slab pull: (1) there are as many advancing trenches as retreating ones, despite the intrinsic negative buoyancy of the slab; and (2) slab age is not, or is even slightly inversely, correlated with trench retreat. Moreover, back-arc spreading associated subduction zones show a very wide range of slab age, from almost 30 My (New Britain) to 110 My (Tonga), that makes it very difficult for the "slab motion-controlled"trench retreat observed for such subductions to be explained by a slab pull influence. Such observations agree with Jarrard (1986) earlier results. The global slab age-dependent trench rollback observed by Garfunkel et al. (1986) may be explained by a combination of various errors, including their back-arc deformation rates (for example, only $30\,\mathrm{mm\,y^{-1}}$ for the Lau basin opening rate) and ocean floor age data, or else introduced by the absolute reference frame (Minster and Jordan, 1978) they used, which is less accurate than HS3-NUVEL1A (e.g., Eurasian plate has opposite absolute motion relative to the Kuril trench). Too much data averaging may also have introduced some errors (only 19 segments are taken into account).

The latter observations disprove the existence of an age-dependent slab rollback and suggest a globally minor slab pull effect on trench motions with respect to the other applied forces, including the pressure force generated on slabs by upper plate motion, the anchoring force, and dynamic local or regional asthenospheric flow. Even under the most favorable conditions for slab pull to affect trench motions, i.e., almost fixed upper plates associated with old slabs, several subduction zones such as Japan ($V_{up(n)} = 20\,mm\,y^{-1}$, slab age = 130 My) or Java ($V_{up(n)} = 15\,mm\,y^{-1}$, slab age = 80 My), do not show any evidence of "slab motion-controlled" back-arc extension: the Japan back-arc is under compression, and Java exhibits a neutral strain regime; both trenches are advancing and more or less follow upper plate motion. The Japan and Sumatra cases may thus attest to spontaneous rollback velocities less than the 15–20 $mm\,y^{-1}$ of the associated upper plates.

To explain back-arc spreading with a dominant "slab motion-controlled" mechanism which is not derived from a slab pull effect, we suggest dynamic asthenospheric flow acting preferentially on one side of the slab. In contrast to the anchoring effect, which only allows a passive resistance of the viscous asthenosphere to the V_{up} limited slab motion, active mantle flow should permit back-arc deformation rates to exceed V_{up} values.

On the basis of various geological and geophysical observations, several authors have advocated a global westward drift of the lithosphere relative to the asthenosphere (Bostrom, 1971; Uyeda and Kanamori, 1979; Ricard et al., 1991; Doglioni, 1993), which might imply the existence of a global relative eastward mantle flow (Nelson and Temple, 1972). The real causes of this phenomenon are not yet fully understood: deceleration of the Earth's rotation, polar wander, tidal drag or consequence of lateral mantle viscosity variations? In any case, if such a global flow exists, it is likely to push slabs in the eastward direction, and would add its effect to the slab anchoring force to favor extension in westward directed subduction zones and compression in eastward directed ones. However, even if there is effectively a quite good correspondence between subduction direction and back-arc deformation style, a global eastward mantle flow influence remains incompatible with motions and deformations at several subduction zones (e.g., the eastward directed and compressive Japan–Kuriles subduction, or the eastward directed and extensional Andaman and New Hebrides subduction zones and their westward directed trench rollback). Such inconsistencies imply mantle flows that locally enhance the single anchoring effect rather than for a global flow influence.

In fact, the existence of local mantle flow (see Fig. 6) has been recognized for Tonga (Smith et al., 2001; Turner and Hawkesworth, 1998) and the Sandwich subduction zones (Russo and Silver, 1994; Pearce et al., 2001; Shemenda, 1994) on the basis of seismological (seismic velocity anisotropy measurements used to estimate mantle flow direction) and geochemical means that allow the affinities of a sub-lithospheric mantle at a particular time and place to be assessed. On the basis of other observations, mantle influences have also been proposed for the New Hebrides (Lagabrielle et al., 1997) and Ryukyu subduction zones (Kubo and Fukuyama, 2003).

Such mantle flows would result from asthenospheric mantle escape, forced out from the diminishing space between converging slabs, favoring material transfer from a shrinking mantle reservoir to an expanding one. It is, for example, well recognized that the subduction zones on the two sides of the Pacific Ocean are globally getting closer to each other (Garfunkel, 1975; Alvarez, 1982; Garfunkel et al., 1986; Lallemand, 1998), implying a shrinking Pacific reservoir from where mantle would tend to escape (note that the idea of a shrinking Pacific do not necessarily implies the general rollback of Pacific margins argued by Garfunkel et al., 1986: roughly, we rather observe, for the last 5–6 My, eastern margins that are retreating faster than western's advance). The Sandwich, Tonga, New Hebrides and New Britain subduction zones are thus likely to be influenced by Pacific mantle reservoir extrusions (Fig. 6). Comparable mechanisms can be invoked for the mantle that underlies the Tibetan region (Tamaki, 1995; Flower et al., 2001). As a consequence of Tethyan closure, this mantle is extruded and thus could be responsible for the westward and southward migration of the Andaman and Ryukyu slabs and associated back-arc openings (Fig. 6).

Mantle escape would be facilitated and preferentially localized in the vicinity of slab leading edges or tears, where lateral mantle flows around the barriers represented by slabs are allowed (Fig. 6). Consequences of such mantle flow localization would be to induce slab rollback near the slab leading edge, generating asymmetrical back-arc extension (Schellart et al., 2002), with decreasing opening rate from one side of the arc (above the slab leading edge) to the other. Three of the six subduction zones that have back-arc deformation rates and trench motions compatible with mantle flow influence (i.e.,Tonga, Ryukyu, and New Hebrides) have been described to be natural examples of asymmetrical back-arc extension (Schellart et al., 2002), with recognized slab leading edge influence. The southern leading edge of the South American subduction seems to be involved in the Sandwich back-arc basin development (Russo and Silver, 1994). To a lesser extent, the Kuril arc undergoes active extension in the north near the tear that cut through the Pacific plate and active compression in the south far from the tear (Yogodzinski et al., 2001).

5. Conclusions

We have illustrated in this study the combined effect of upper plate absolute motion and local and/or regional asthenospheric flow to control tectonic stress in the arc/back-arc system. The so-called anchoring-force, aimed to resist slab migration, could be effective but is almost never fully efficient. The age-dependent slab pull force contributes either slightly or not at all to trench retreat that could explain back-arc extension. The magnitude of the slab pull force is certainly the most easy to estimate because slab mean densities and ages are roughly known for most areas. The other forces acting on slabs like the anchoring force, the pressure transmitted from upper plate motion, or the asthenospheric flow forces are much more difficult to estimate, because they depend on the viscosity of the mantle surrounding the slabs which is very poorly constrained. We thus hope to constrain these forces by examining their effect on the upper plate tectonic stress and deformation rates. We already know from this study that their effect is larger than those generated from the bending moment of the slab pull.

Acknowledgements

We warmly thank D. Boutelier, S. Dominguez, E. Calais, Y. Font and J.-Y. Royer for their help and advice in data extraction, and K. Otsuki, R.M. Russo and S. King for their careful and useful comments in review that helped improve the manuscript.

References

Alvarez, W., 1982. Geological evidence for the geographical pattern of return flow and the driving mechanism of plate tectonics. J. Geophys. Res. 87, 6697–6710.

Bostrom, R.C., 1971. Westward displacement of the lithosphere. Nature 234, 536–538.

Carlson, R.L., Hilde, T.W.C., Uyeda, S., 1983. The driving mechanism of plate tectonics: Relation to age of the lithosphere at trench. Geophys. Res. Lett. 10, 297–300.

Carlson, R.L., Melia, P.J., 1984. Subduction hinge migration. In: Carlson, R.L., Kobayashi, K. (Eds.), Tectonophysics, vol. 102. pp. 1–16.

Carlson, R.L., Mortera-Gutiérrez, C.A., 1990. Subduction hinge migration along the Izu-Bonin-Mariana arc. Tectonophysics 181, 331–344.

Chamot-Rooke, N., 2001. Timing and Opening of Andaman Basin Opening. AGU, Boston.

Chamot-Rooke, N., Vigny, C., Rangin, C., Walpersdorf, A., Le Pichon, X., Huchon, P., 1997. Sundaland motion detected from Geodyssea GPS measurement part 1: implication for motion at Sunda trench. In: Geodyssea (Geodynamics of the South and Southeast Asia) Concluding Symposium, Penang, Malaysia 14–18 April (Abstract).

Chapple, W.M., Tullis, T.E., 1967-1984. Evaluation of the forces that drive the plates. J. Geophys. Res. 82.

Chase, C.G., 1978. Plate kinematics: the America, East Africa, and the rest of the world. Earth Planet. Sci. Lett. 37, 355–368.

Demets, C., Gordon, R.G., Argus, D.F., Stein, S., 1994. Effect of recent revisions to the geomagnetic reversal time scale on estimates of current plate motion. Geophys. Res. Lett. 21, 2191–2194.

Dewey, J.F., 1980. Episodicity, sequence and style at convergent plate boundaries. In: D., Strangway, (Ed.). The Continental Crust and Its Mineral Deposits. Geol. Assoc. Can., Spec. Pap. 20, pp. 553–573.

Doglioni, C., 1993. Geological evidence for a global tectonic polarity. J. Geol. Soc. Lond. 150, 991–1002.

Dvorkin, J., Nur, A., Mavko, G., Ben-Avraham, Z., 1993. Narrow subducting slabs and the origin of back-arc basins. Tectonophysics 227, 63–79.

Engdahl, R., van der Hilst, R., Buland, R., 1998. Global teleseismic earthquake relocation with improved travel times and procedures for depth determination. Bull. Seism. Soc. Am. 88, 722–743.

Flower, M.F.J., Russo, R.M., Tamaki, K., Hoang, N., 2001. Mantle contamination and the Izu-Bonin-Mariana (IBM) 'high-tide mark': evidence for mantle extrusion caused by Tethyan closure. Tectonophysics 333, 9–34.

Forsyth, D.W., Uyeda, S., 1975. On the relative importance of the driving forces of plate motion. Geophys. J. Royal Astronomical Soc. 43, 163–200.

Freymuller, J.T., Kellog, J.N., VEGA, V., 1993. Plate motions in the North Andean region. J. Geophys. Res. 98, 21853–21863.

Garfunkel, Z., 1975. Growth, shrinking, and long-term evolution of plates and their implication for the flow pattern in the mantle. J. Geophys. Res. 80, 4425–4432.

Garfunkel, Z., Anderson, C.A., Schubert, G., 1986. Mantle circulation and the lateral migration of subducted slabs. J. Geophys. Res. 91, 7205–7223.

Gripp, A.E., Gordon, R.G., 1990. Current plate velocities relative to the hot spots incorporating the NUVEL-1 global plate motion model. Geophys. Res. Lett. 17, 1109–1112.

Gripp, A.E., Gordon, R.G., 2002. Young tracks of hot spots and current plate velocities. Geophys. J. Int. 150, 321–361.

Heki, K., Miyazaki, S., Takahashi, H., Kasahara, M., Kimata, F., Miura, S., Vasilenko, N.F., Ivashchenko, A., An, K.-D., 1999. The Amurian Plate motion and current plate kinematics in eastern Asia. J. Geophys. Res. 104, 29147–29155.

Hyndman, R.D., 1972. Plate motions relative to the deep mantle and the development of subduction zones. Nature 238, 263–265.

Jarrard, R.D., 1986. Relations among subduction parameters. Rev. Geophys. 24, 217–284.

Jolivet, L., 1995. La déformation des continents: exemples régionaux. Hermann, Editeurs des Sciences et des Arts. Collection Enseignement des Sciences.

Klotz, J., Khazaradze, G., Angermann, D., Reigber, C., Perdomo, R., Cifuentes, O., 2001. Earthquake cycles dominates contemporary crustal deformation in Central and Southern Andes. Earth Planet. Sci. Lett. 193, 437–446.

Kubo, A., Fukuyama, E., 2003. Stress field along the Ryukyu Arc and the Okinawa Trough inferred from moment tensors of shallow earthquakes. Earth Planet. Sci. Lett. 210, 305–316.

Lagabrielle, Y., Goslin, J., Martin, H., Thirot, J.-L., Auzende, J.-M., 1997. Multiple active spreading centers in the hot North Fiji Basin (Southwest Pacific): a possible model for Archean seafloor dynamics? Earth Planet. Sci. Lett. 149, 1–13.

Lallemand, S., 1995. High rates of arc consumption by subduction processes; some consequences. Geology 23, 551–554.

Lallemand, S., 1998. Possible interaction between mantle dynamics and high rates of consumption by subduction process in circum-Pacific area. Geodynamics 27, 1–9.

Martinez, F., Becker, N., Freyer, P., 2000. Geophysical characteristics of the southern Mariana trough, 11°59′N–13°40′N. J. Geophys. Res. 105, 16591–16607.

Mazzotti, S., 1999. L'arc insulaire japonais : déformation transitoire et permanente liée à la subduction et à la collision. Ph.D. Thesis, Université Paris-Sud, Orsay-Paris XI.

Mazzotti, S., Henry, P., Le Pichon, X., 2001. Transient and permanent deformation of central Japan estimated by GPS. 2. strain partitioning and arc-arc collision. Earth Planet. Sci. Lett. 184, 455–469.

Minster, J.B., Jordan, T.H., 1978. Present-day plate motions. J. Geophys. Res. 83, 5331–5354.

Molnar, P., Atwater, T., 1978. Interarc spreading and Cordilleran tectonics as alternates related to the age of subducted oceanic lithosphere. Earth Planet. Sci. Lett. 41, 330–340.

Müller, R., Roest, W., Royer, J.-Y., Gahagan, L., Sclater, J., 1997. Digital isochrons of the world's ocean floor. J. Geophys. Res. 104, 3211–3214.

Miyasaki, S., Matsuzaka, S., Heki, K., Kaidzu, M., Kuroishi, Y., Murakami, M., Imakiire, T., Tada, T., Nitta, K., Nakagawa, H., Itabashi, A., Karasawa, M., Ootaki, O., Ishikawa, N., Ishimoto, M., Takahashi, H., Kasahara, M., An, K.-D., 2001. Tectonics in the Eastern Asia inferred from GPS observations. Bull. Geograph. Surv. Inst. 47, 1–12.

Nelson, T.H., Temple, P.G., 1972. Mainstream mantle convection: a geologic analysis of plate motion. Am. Assoc. Petrol. Geol. Bull. 56, 226–246.

Otsuki, K., 1989. Empirical relationships among the convergence rate of plates, rollback rate of trench axis and island-arc tectonics: laws of convergence rates of plates. Tectonophysics 159, 73–94.

Oxburgh, R., Turcotte, D., 1974. Origin of paired metamorphic belts and crustal dilatation in island arc regions. J. Geophys. Res. 76, 1325–1327.

Pearce, J.A., Leat, P.T., Barker, P.F., Millar, I.L., 2001. Geochemical tracing of Pacific-to-Atlantic upper-mantle flow through the Drake passage. Nature 410, 457–461.

Pelletier, B., Calmant, S., Pillet, R., 1998. Current tectonics of the Tonga–New Hebrides region. Earth Planet. Sci. Lett. 164, 263–276.

Rangin, C., Le Pichon, X., Mazotti, S., Pubellier, M., Chamot-Rooke, N., Aurelio, M., Walpersdorf, A., Quebral, R., 1999. Plate convergence measured by GPS across the Sundaland/Philippine Sea Plate deformed boundary: the Philippines and eastern Indonesia. Geophys. J. Int. 139, 296–316.

Ricard, Y., Doglioni, C., Sabadini, R., 1991. Differential rotation between lithosphere and mantle: a consequence of lateral viscosity variations. J. Geophys. Res. 96, 8407–8415.

Russo, R.M., Silver, P.G., 1994. Trench-parallel flow beneath the Nazca plate from seismic anisotropy. Science 263, 1105–1111.

Schellart, W.P., Lister, G.S., Jessell, M.W., 2002. Analogue modelling of assymetrical back-arc extension. J. Virtual Explorer 7, 25–42.

Scholz, C.H., Campos, J., 1995. On the mechanism of seismic decoupling and back-arc spreading at subduction zones. J. Geophys. Res. 100, 22103–22115.

Shemenda, A.I., 1994. Subduction: Insights from Physical Modeling. Kluwer Academic Publishers, Dordrecht.

Sleep, N., Toksöz, M., 1971. Evolution of marginal basins. Nature 33, 548–550.

Smith, G.P., Wiens, D.A., Fischer, K.M., Dorman, L.M., Webb, S.C., Hildebrand, J.A., 2001. A complex pattern of mantle flow in the Lau back-arc. Science 292, 713–716.

Tamaki, K., 1995. Upper mantle extrusion tectonics of southeast Asia and formation of western Pacific back-arc basins. In: International Workshop: Cenozoic Evolution of the Indochina Peninsula, Hanoi/Do Son, April 1995, 89 pp., Abstract with programs.

Tregoning, P., 2002. Plate kinematics in the western Pacific derived from geodetic observations. J. Geophys. Res. 107, 1–8, ECV7.

Tregoning, P., Lambeck, K., Stolz, A., Morgan, P., McClusky, S.C., van der Beck, P., McQueen, H., Jackson, R.J., Little, R.P., Laing, A., Murphy, B., 1998. Estimation of current plate motions in Papua New Guinea from Global Positioning System observations. J. Geophys. Res. 103, 12181–12203.

Tregoning, P., Jackson, J.J., McQueen, H., Lambeck, K., Stevens, C., Little, R.P., Curley, R., Rosa, R., 1999. Motion of the South Bismarck plate Papua New Guinea. Geophys. Res. Lett. 26, 3517–3520.

Turner, S., Hawkesworth, C., 1998. Using geochemistry to map mantle flow beneath the Lau basin. Geology 26, 175–183.

Uyeda, S., 1982. Subduction zones: an introduction to comparative subductology. Tectonophysics 81, 133–159.

Uyeda, S., Kanamori, H., 1979. Back-arc opening and the mode of subduction. J. Geophys. Res. 84, 1049–1061.

Vanneste, L.E., Larther, R.D., Smythe, D.K., 2002. A slice of intraoceanic arc: insight from the first multichannel seismic reflexion profile across the South Sandwich Island arc. Geology 30, 819–822.

Yogodzinski, G.M., Lees, J.M., Churikova, T.G., Dorendorf, F., Woerner, G., Volynets, O.N., 2001. Geochemical evidence for the melting of subducting oceanic lithosphere at plate edges. Nature 409, 500–504.

Yu, S.B., Kuo, L.C., 1996. GPS observations of crustal deformation in the Taiwan-Luzon region. Geophys. Res. Lett. 26, 923–926.

Zellmer, K.E., Taylor, B., 2001. A three plate kinematic model for Lau Basin opening. Geochemistry, Geophysics and Geosystems 2, paper no. 2000GC000106.